IOPscience iopscience.iop.org

Home Search Collections Journals About Contact us My IOPscience

Magnetotransport in epitaxial films of the degenerate semiconductor $Zn_{1-x}Co_xO$

This article has been downloaded from IOPscience. Please scroll down to see the full text article.

2005 J. Phys.: Condens. Matter 17 75

(http://iopscience.iop.org/0953-8984/17/1/008)

View the table of contents for this issue, or go to the journal homepage for more

Download details:
IP Address: 129.252.86.83
The article was downloaded on 27/05/2010 at 19:30

Please note that terms and conditions apply.

INSTITUTE OF PHYSICS PUBLISHING JOURNAL OF PHYSICS: CONDENSED MATTER

J. Phys.: Condens. Matter **17** (2005) 75–86 doi:10.1088/0953-8984/17/1/008

Magnetotransport in epitaxial films of the degenerate semiconductor $Zn_{1-x}Co_xO$

R C Budhani[1,3], Prita Pant[1], R K Rakshit[1], K Senapati[1], S Mandal[1], N K Pandey[1] and Jitendra Kumar[2]

[1] Department of Physics, Indian Institute of Technology Kanpur, Kanpur-208016, India
[2] Materials Science Programme, Indian Institute of Technology Kanpur, Kanpur-208016, India

E-mail: rcb@iitk.ac.in

Received 18 October 2004, in final form 25 November 2004
Published 10 December 2004
Online at stacks.iop.org/JPhysCM/17/75

Abstract

Magnetotransport measurements are performed over a broad range of temperature (T) and magnetic field (H) on highly degenerate n-type $Zn_{1-x}Co_xO$ ($0 \leqslant x \leqslant 0.30$) epitaxial films. The cobalt-free samples are characterized by a metallic resistivity $\rho(T)$ down to 2 K, a negative and predominantly isotropic magnetoresistance (MR) and optical transmission above 85% in the visible range of the electromagnetic spectrum. X-ray diffraction measurements show that while for $x \leqslant 0.20$, all cobalt atoms occupy the tetrahedral sites of the wurtzite structure of ZnO, a phase separation into CoO is seen for $x > 0.2$. In the solution phase, we do not observe any signatures of a spontaneous ordering of the cobalt spins despite a large concentration of mobile electrons ($>10^{20}$ cm^{-3}). The absence of anomalous Hall resistance is consistent with this observation. The carrier concentration (n) over the entire range of x remains above the Mott limit for the insulator-to-metal transition in a doped semiconductor. However, while the Co-free samples are metallic ($T > 2$ K), we see a resistivity (ρ) minimum followed by ln T divergence of $\rho(T)$ at low temperatures with increasing x. The magnetoresistance of these samples is negative and predominantly isotropic. Moreover, the MR tends to follow a log H behaviour at high fields. These observations, including the Kondo-like minimum in the resistivity, suggest s–d exchange dominated transport in these dilute magnetic semiconductors.

1. Introduction

The prospects for making a dilute magnetic semiconductor (DMS) out of ZnO by substitutional doping with transition metals have led to several studies directed towards synthesis of thin films and bulk samples of $Zn_{1-x}T_{mx}O$, where T_m is Cr, Mn, Fe, Co or Ni [1]. While signatures of

[3] Author to whom any correspondence should be addressed.

0953-8984/05/010075+12$30.00 © 2005 IOP Publishing Ltd Printed in the UK

a long range ferromagnetic order setting in at temperatures well above 300 K have been seen in many cases [1–7], there is a fair amount of debate on the origin of this magnetic order [8–12]. In some cases it has been shown that the magnetism is related to isolated clusters of the transition metal or clusters of its oxides, whereas in others, a seemingly homogeneous solid solution orders due to the alignment of 3d spins at the transition metal ion sites. There are four fundamental questions that one has to address in order to fully understand the magnetic state of these oxides. These are:

(i) the solubility limit of the transition metal ions in the wurtzite lattice of ZnO;
(ii) limitations on the Ruderman–Kittel–Kasuya–Yosida-type (RKKY-type) [1] mobile-carrier-assisted ordering of the transition metal moments;
(iii) in the absence of mobile carriers, the required minimum distance between the T_m ions (required minimum solubility) for magnetic ordering; and, finally,
(iv) manifestations of the magnetic moments, ordered or otherwise, in magnetotransport properties of the DMS.

In the context of the technological importance of these semiconductors, it is also important to know the effects of magnetic impurities on the band gap, defect states and excitonic levels of this wide band gap semiconductor.

A non-equilibrium method for incorporating larger amounts of transition metal ions in the ZnO lattice is through the thin film route. There are several reports on thin films of ZnO doped with Co prepared using pulsed laser deposition (PLD) and sputtering [1–5]. A consistently larger solubility of Co, compared to the solubility in bulk samples, is seen in thin films deposited at $T < 600\,^{\circ}$C. However, there are conflicting reports on the magnetic character of these films. While no intrinsic ferromagnetism was found in several studies [1, 11, 12], results of Ueda *et al* [2] on PLD films of Al doped $Zn_{1-x}Co_xO$ are remarkably different. A large n-type carrier density ($\sim 2.9 \times 10^{20}$ cm^{-3} for $x = 0.15$) induced by aluminium doping seems to result in room temperature ferromagnetism in these films. The first-principles density functional calculations of Lee and Chang [13] also predict room temperature ferromagnetism in electron doped $Zn_{1-x}Co_xO$. There are also reports of ferromagnetism in films where no third group element has been introduced for n-type doping [3, 4]. These films presumably have a low electron concentration originating from the oxygen related defects. A true test of ferromagnetism resulting from long range ordering of the Co spins in the ZnO lattice, however, requires a careful separation of the effects of nanoscale phase separation of cobalt rich phases. The authentic ferromagnetic state will have its signatures in the Hall conductivity, magnetoresistance and magnetic circular dichroism. Such detailed studies of electron transport in cobalt doped ZnO films are, however, lacking.

We therefore felt it desirable to undertake a systematic study of the solubility limit of Co in electron doped ZnO films and measure their conductivity, Hall resistivity and magnetoresistance over a broad range of temperature, magnetic field and cobalt concentration. While there is no evidence of a carrier-mediated ferromagnetism in the Hall and magnetization data of these samples, interesting effects of s–d exchange are seen in the magnetoresistance and resistivity, which include a Kondo-like anomaly at low temperatures. These films provide a model system for studying s–d exchange at moderate carrier densities.

2. Experimental details

Polycrystalline targets of general formula $[(ZnO)_{0.99}(Al_2O_3)_{0.01}]_{(1-x)}(CoO)_x$ were first synthesized following the standard solid-state technique route [10]. The required powders (ZnO, Al_2O_3, Co_3O_4), were taken in stoichiometric proportions, thoroughly mixed and ground

together for one hour and then annealed at a temperature of 1150 °C for ∼12 h. This process was repeated three times to ensure mixing of cations at the atomic level. The powder samples were subsequently pelletized in the form of 22 mm diameter and ∼6 mm thick discs using a hydraulic press. These pellets were finally sintered at 1300 °C for ∼12 h.

An excimer laser based ($\lambda = 248$ nm) PLD set-up [14] was used to deposit ∼2500–5000 Å films on optically flat (0001) sapphire plates in vacuum ($\sim 5 \times 10^{-6}$ Torr) at 600 °C. X-ray diffraction studies were carried out in the standard Bragg–Brentano geometry with a Cu Kα source. Magnetization measurements were performed on 5×10 mm^2 samples using a superconducting quantum interference device (SQUID) based magnetometer (Quantum Design MPMS-XL5) over a wide range of temperature and magnetic field strength. The magnetization signal was carefully corrected for the diamagnetic contribution from the substrate which is quite large at high fields. Measurements of resistivity $\rho_{xx}(T)$, Hall coefficient (R_{H}) and magnetoresistance (MR) were carried out on samples deposited in the form of a six-probe Hall bar geometry through a stainless steel shadow mask. A low frequency ac technique was used for the transport measurements down to liquid helium temperatures and in magnetic field up to 10 T. While in most of the MR measurements the magnetic field was perpendicular to the plane of the film (orbital geometry), some low field measurements were carried out with the field in the plane of the film and parallel to the direction of the measuring current (the Lorentz-force-free configuration).

3. Results

The x-ray θ–2θ diffraction patterns of four films with the Co concentrations $x = 0, 0.10, 0.20$ and 0.30 are shown in figure 1. In samples with $x \leqslant 0.20$ we see only the diffraction peaks corresponding to the (0002) and (0004) reflections of the wurtzite structure, in addition to the reflections from the single-crystal substrate. From these data, it is clear that the film maintains epitaxial registry with the structure of the underlying substrate. In the sample with $x = 0.30$, two weak (note the logarithmic scale) additional reflections appear at $2\theta = 36.51°$ and 77.49°. These can be identified with the (111) and (222) reflections of the cubic phase of CoO. In fact, signatures of the presence of the CoO phase are also seen in samples with $x = 0.25$. These results indicate that within the resolution limit of x-ray diffraction, the upper limit of solubility of Co in ZnO is $\leqslant$20%. Since the total electron density in CoO (cubic NaCl type) is higher by a factor of ∼15% as compared to the electron density in wurtzite ZnO, we believe that even nanoscale phase separation of CoO would be detectable with x-ray diffraction.

A strong diamagnetic response of the sapphire substrate makes the measurements of magnetization in thin film samples of $Zn_{1-x}Co_xO$ quite non-trivial. To illustrate this point, in panel (a) of figure 2 we show the M–H curve for a bare substrate from the same lot on which films were deposited. A large diamagnetic response ($\sim -2 \times 10^{-4}$ emu g^{-1} at ∼500 Oe) is evident in the figure. We have subtracted the emu g^{-1} signal of the substrate from the emu g^{-1} signal of the substrate plus film system to extract the contribution of the film. These data are shown in panels (b) and (c) of figure 2 for the samples with $x = 0.20$ and 0.30. The response of the sample with $x = 0.10$ is similar to the data shown in panel (b). A linear dependence of magnetization on field within the uncertainty of these measurements suggests that these samples are devoid of any long range ferromagnetic order. For the sample with $x = 0.30$, we notice a slight deviation from linearity in the field range of 0–300 Oe, which can be attributed to uncompensated spins on the surface of antiferromagnetic CoO particles. As pointed out by Néel, this results from imperfect compensation of magnetic sublattices [15].

Results of electrical resistivity measurements over the temperature range of 2–315 K for the samples with $x = 0$, 0.10, 0.20 and 0.30 are shown in figure 3. The resistivity of

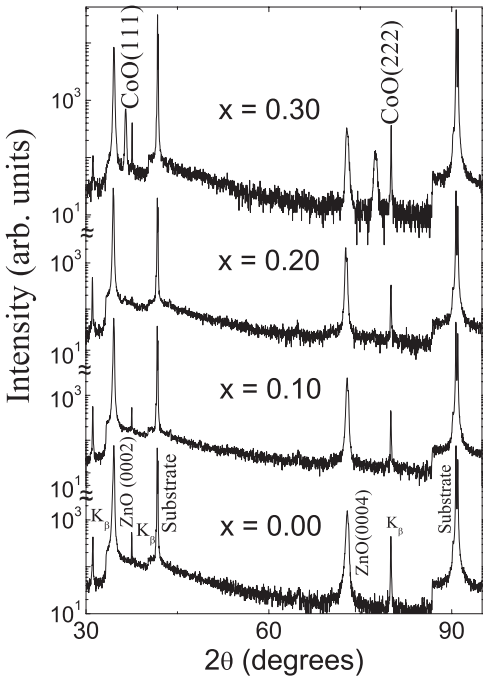

Figure 1. The $Cu_{K\alpha}$ x-ray diffraction pattern of the $Zn_{1-x}Co_xO$ films deposited on (0001) sapphire substrates. Diffractograms for the samples with $x = 0.0$, 0.10, 0.20 and 0.30 are shown. The *hkl* values of the wurtzite structure and of the impurity phase CoO are marked in the figure.

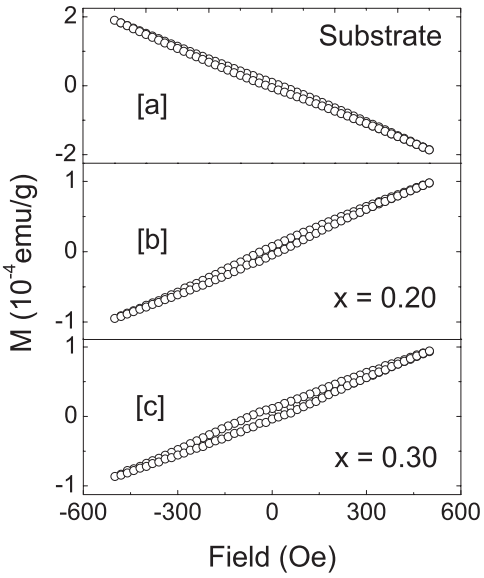

Figure 2. Zero-field cooled magnetization curves at 10 K for a bare substrate (panel (a)), film with $x = 0.20$ (panel (b)) and film with $x = 0.30$ (panel (c)). The magnetic field in these measurements was in the plane of the substrate.

the cobalt-free sample is the lowest ($\rho_{xx}(300\ \mathrm{K}) \approx 1.0\ \mathrm{m\Omega\ cm^{-1}}$), and it remains metallic (positive $\mathrm{d}\rho_{xx}/\mathrm{d}T$) over the entire temperature range. In spite of its metallic conductivity, the material is highly transmissive for the visible light with the transmission coefficient for 500 nm wavelength being as high as 85%. Needless to say, these films present examples of an excellent transparent conductor [16, 17]. The room temperature resistivity of the samples increases with the cobalt content, first slowly and then rapidly, as is evident in the inset of figure 3. The temperature dependence of the resistivity of the samples with $x > 0.10$ also shows an upturn at lower temperatures, which becomes pronounced in the sample with $x = 0.30$. While a definitive statement on the ground state (metallic or insulating) of these samples requires measurements at still lower temperatures, we will argue that this upturn is a manifestation of the s–d scattering dominated transport in cobalt substituted samples.

In figures 4(a)–(c) respectively we show the variation of the Hall resistivity (ρ_{xy}) with applied magnetic field for samples with $x = 0$, 0.20 and 0.30 at several temperatures. For the cobalt-free sample (panel (a)), the Hall resistance increases linearly with the field and the slope of the ρ_{xy} versus H curves shows a small but distinct increase with temperature. To illustrate this point, in the inset of each panel we have plotted $\Delta\rho_{xy}$ ($=\rho_{xy}(T, H) - \rho_{xy}(10\ \mathrm{K}, H)$) as a function of field. The linear dependence of $\rho_{xy}(T, H)$ on the field is preserved in the case of the cobalt substituted samples as well, albeit with some differences in the slope and the temperature dependence of the slope. In a substance with long range ferromagnetic order, the Hall resistivity varies as $\rho_{xy} = R_0(T)H + R_s(T)\mu_0 M(T, H)$, where μ_0 and $M(T, H)$

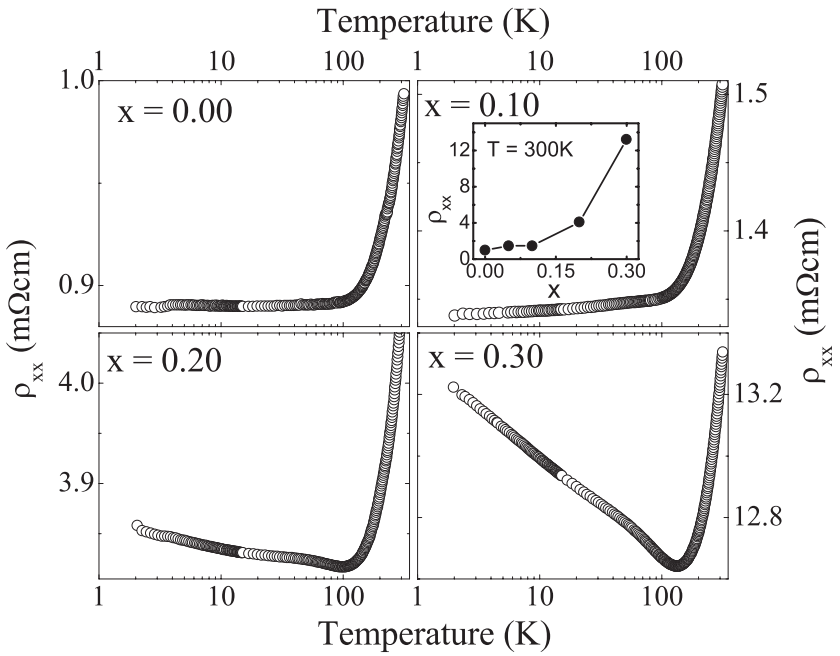

Figure 3. The zero-field longitudinal resistivity ($\rho(T)$) of the films with $x = 0.0$, 0.10, 0.20 and 0.30 plotted as a function of temperature. The inset shows the variation of the room temperature resistivity as a function of the cobalt concentration.

are the magnetic permeability and magnetization respectively and $R_0(T)$ is the ordinary Hall coefficient representing non-magnetic scattering of the charge carriers subjected to a Lorentz force [18, 19]. For single-band conduction following degenerate statistics, $R_0(T) = 1/nec$, where n is the carrier concentration. The coefficient $R_s(T)$ arises from the side jump mechanism [20] and asymmetric scattering [21] of conduction electrons from the centre of the magnetic impurity potential. The magnitude of this anomalous contribution to the Hall effect depends on the strength of the spin–orbit interaction of the conduction electrons as they go around the magnetic impurity, and the relative number of the up and down spin electrons in the spin-split conduction band. For a ferromagnetically ordered substance, ρ_{xy} increases rapidly with field until the magnetization reaches its saturation value, and any subsequent growth of the ρ_{xy} is determined by the first term, which is linear in field. The dependence of $R_s(T)$ on the longitudinal resistivity ρ_{xx} is of the form $R_s(T) \sim \rho_{xx}^n$, with the n varying from 1 to 2 [19]. The monotonic increase of ρ_{xy} for all samples, as seen in figures 4(a)–(c), clearly indicates the absence of a long range ferromagnetic order in these samples.

In figures 5(a) and (b) respectively, we plot the variation of the carrier concentration (n) and Hall mobility (μ_H) as a function of temperature for all samples. While n is $\approx 2 \times 10^{20}$ cm^{-3} for the cobalt-free sample, it is evident that incorporation of Co in the films causes a marginal reduction in n. We also see a drop in the mobility of the carriers on substitution of cobalt.

A key transport property of dilute magnetic semiconductors, which reflects various facets of the potential landscape originating from impurities, moment carrying sites, lattice disorder and electron–electron interactions, is the magnetoresistance. In figure 6(a) we present the MR data for the cobalt-free sample. The magnetoresistance in the temperature range investigated here (10 K $< T <$ 200 K) remains negative as the field is scanned from zero to 100 kOe. The

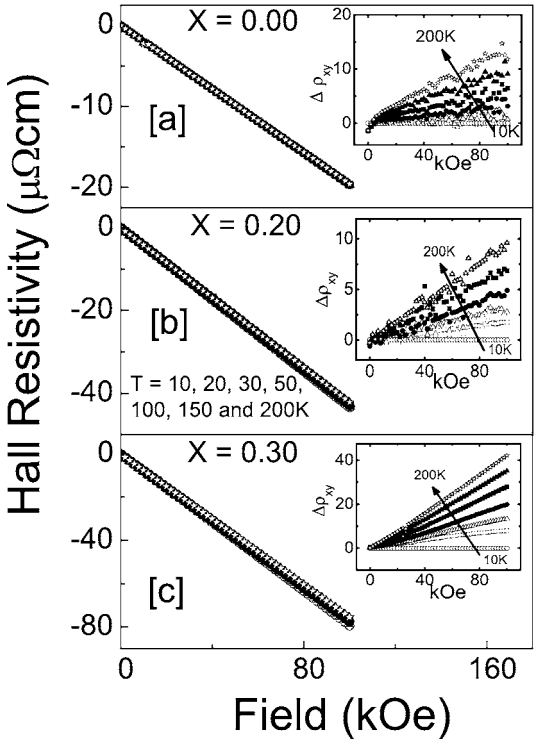

Figure 4. (a)–(c): Hall resistivity ρ_{xy} is plotted as a function of magnetic field. Data for samples with $x = 0.00$, 0.20 and 0.30 are shown in panels (a), (b) and (c) respectively. The measurements were performed at several temperatures as indicated in the figures. In order to highlight the changes in ρ_{xy} with temperature, in the inset of each figure we have plotted $\Delta\rho_{xy}$ ($\rho_{xy}(T, H) - \rho_{xy}(10\ \mathrm{K}, H)$).

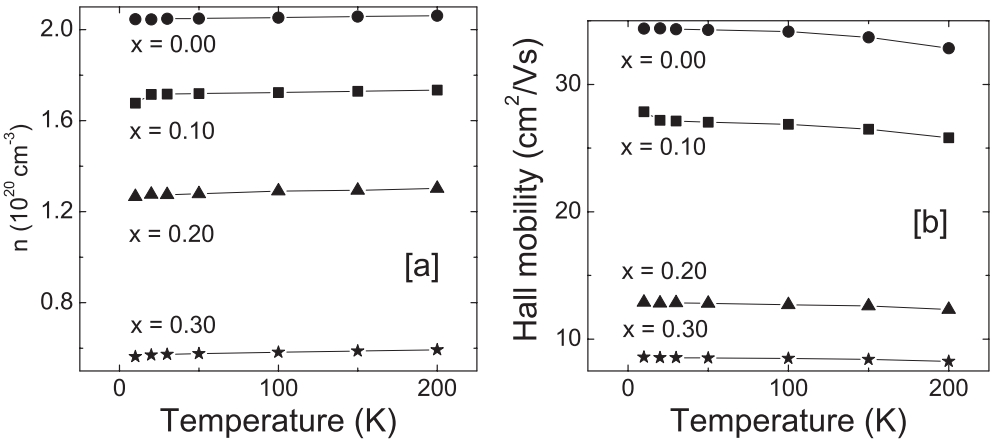

Figure 5. (a), (b): the variation of the carrier concentration (n) and the Hall mobility (μ_{H}) as a function of temperature is plotted in panel (a) and panel (b) respectively for the samples with $x = 0.00$, 0.20 and 0.30. Solid lines in the figures are guides to the eye.

field dependence is rapid at the beginning and then a log H behaviour follows at large fields. Further, the MR is quenched at higher temperatures at each value of the field. The temperature and field dependence of the MR seen in figure 6(a) is typical of a semiconductor doped well beyond the Mott limit [22, 23] on carrier concentration for insulator-to-metal transition, which is given as

$$n_{\mathrm{c}} = (0.26/a_{\mathrm{H}})^3. \tag{1}$$

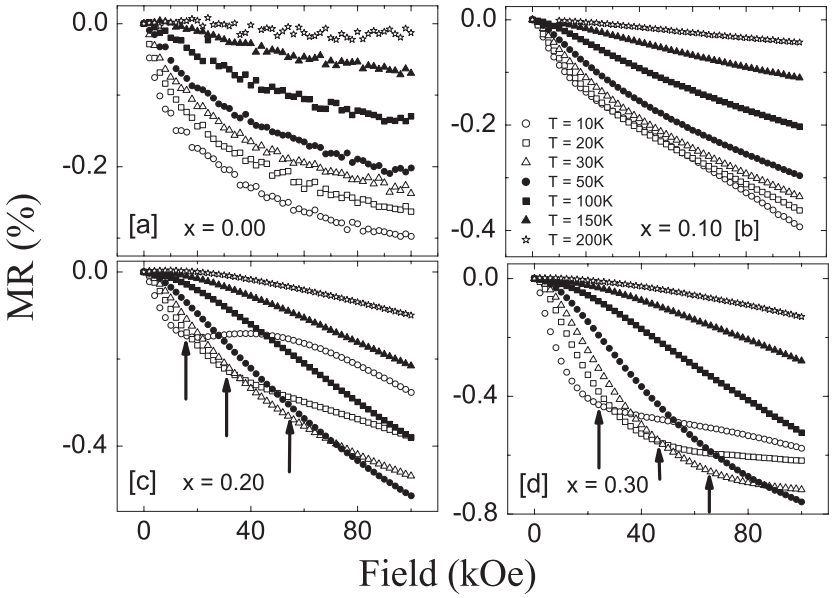

Figure 6. (a)–(d): the transverse magnetoresistance $\Delta\rho/\rho[\{\rho(H) - \rho(0)\}/\rho(0)]$ at several temperatures of the film with $x = 0.00$, 0.10, 0.20 and 0.30 is plotted as a function of magnetic field in panels (a) to (d) respectively. The direction of the field in all cases was perpendicular to the plane of the film and perpendicular to the direction of the measuring current. Arrows in the figures mark the critical field H^* (see the text).

Here $a_{\rm H} = \varepsilon\hbar^2/m^*e^2$ is the effective Bohr radius of the donor. With the effective mass m^* and dielectric constant ε taking values of 0.38 $m_{\rm e}$ and 8.5 respectively for ZnO [24], the donor radius is $\approx$12 Å and $n_{\rm c} = 1.1 \times 10^{19}$ cm^{-3}. The measured carrier concentration in cobalt-free ZnO films (2×10^{20} cm^{-3}) far exceeds the Mott limit. For this heavily degenerate semiconductor, it is fair to argue that the Fermi level is in the conduction band.

While the qualitative behaviour of MR with temperature and field in the sample with 10% cobalt (figure 6(b)) is similar to that of the cobalt-free sample, a progressively different behaviour emerges with increasing cobalt concentration. For example, in the sample with $x = 0.20$, the MR at 10 K first increased rapidly and then reached a plateau at a critical field H^* indicated by an arrow in figures 6(c) and (d). We also note that this critical field increases with temperature. The absolute values of the MR and H^* at each temperature are higher for the sample with 30% cobalt (figure 6(d)). In fact, some vestiges of this behaviour are also seen for the sample with $x = 0.10$.

An interesting behaviour of the MR emerges when the magnetic field is aligned parallel to the plane of the film and in the direction of the measuring current. Figure 7(a) shows the data for the cobalt-free sample at 10 K. While there is a small difference ($\sim$11% at the highest field) between the parallel and perpendicular configurations, the MR is predominantly isotropic. A similar behaviour of the MR is seen for the sample with 30% cobalt (figure 7(b)).

4. Discussion

The metallic conduction observed in the cobalt-free samples over the entire temperature range is consistent with the measured carrier concentration of $\sim 2 \times 10^{20}$ cm^{-3}, which is well beyond the Mott criterion for the insulator-to-metal transition in a doped semiconductor. Further, if we

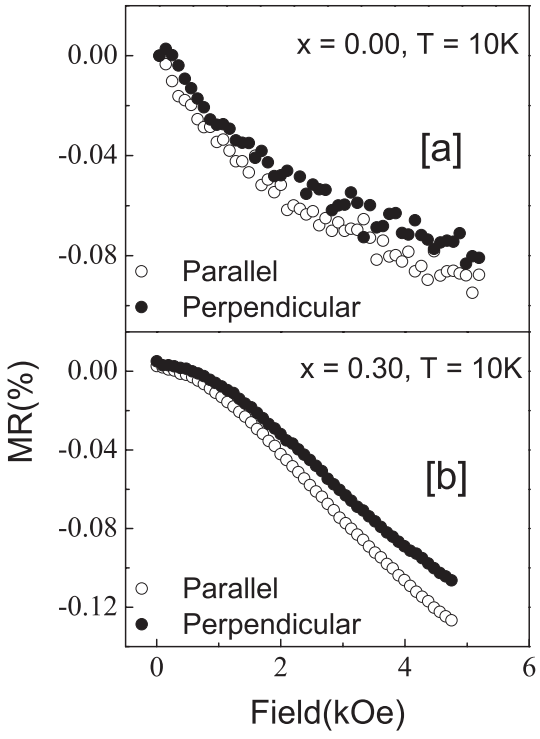

Figure 7. (a) and (b): panel (a) shows the low field MR of the cobalt-free sample ($x = 0.00$) for two orientations of the magnetic field: in one case the field was perpendicular to the plane of the film and in the other it was in the plane and parallel to the direction of the current; panel (b) shows results of the same measurement performed on a film with $x = 0.30$.

assume that the conduction band has a single minimum in the Brillouin zone, and the band is spherical near the minimum, we get a Fermi energy ($E_F = (\hbar^2/2m^*)(3\pi^2 n)^{2/3}$) of ∼320 meV for the $x = 0$ sample. From the known m^* and measured n, we have extracted the Ioffe–Regel number $k_F l$. This disorder parameter varies from 8 to 1 as we increase x from 0.0 to 0.3. Since $k_F l$ is $\geqslant 1$ in all cases, these samples can be considered metallic.

Like most degenerate semiconductors [24], the magnetoresistance of our cobalt-free ZnO samples is negative. Mapping the problem of MR in heavily doped semiconductors onto the problem of negative MR in Cu:Mn alloys [25] with localized magnetic moments at Mn sites, Toyozawa [26] argued that localized moments originating from fluctuations in the mobile carrier density in doped semiconductors can lead to a similar effect. If the magnetization due to the localized moments is M, the transport then consists of two parallel channels, one with resistivity $\rho_{xx1}(H) \propto (1 + cM)$ for conduction electrons with their spins parallel to M and the other with $\rho_{xx2}(H) \propto (1 - cM)$ for electrons with antiparallel spins [23]. The resulting MR is $\Delta\rho/\rho \propto (-M)^2$. Considering a linear magnetic response of the localized spins, the MR is expected to scale with the square of the applied magnetic field. We have attempted to fit the MR data to an empirical expression of the type $\Delta\rho/\rho \sim H^n$. The value of the power extracted from these fits ranges from 0.6 to 1.3 in the low field region as the temperature is increased from 10 to 200 K. This type of deviation from a quadratic dependence on H has been seen in a large number of doped semiconductors with carrier concentration above the Mott limit [23, 27].

In a low carrier density disordered system, one might expect to see manifestations of weak localization and electron–electron interaction effects in the resistivity and MR. In 2D, electron–electron interaction effects lead to a positive MR at low temperatures [28]. In the weak localization limit, a constructive interference between electron trajectories when a magnetic

field is applied perpendicular to the plane of the film leads to a negative MR [28, 29]. The sign and orientation dependence of the MR in the present case is not consistent with the predictions for these quantum corrections. Furthermore, the resistivity of our cobalt-free samples is metallic down to ∼2 K, whereas a $\ln T$ divergence of ρ is expected for the e–e and localization effects. The temperature dependence of the resistivity also deviates from the predictions for localization and interaction effects in a 3D system [28–30].

The concept of scattering of mobile carriers by localized spins has a strong basis in the case of the cobalt substituted samples. In the composition range where all cobalt atoms replace Zn sites in the wurtzite lattice, each Co^{2+} ion is surrounded by four oxygen ions situated on the corners of a tetrahedron. In the presence of this tetrahedral crystal field, the free ion ^{4}F ground state would split into a $^4A_2$ orbital singlet ($S = 3/2$), which is the new ground state, and two orbital triplets located at much higher energies as in the case of wurtzite $Cd_{1-x}Co_xSe$ [31, 32]. The magnetic moment $g\mu_B[S(S+1)]^{1/2}$ associated with the cobalt ions, and the proximity of the d levels to the Fermi energy, provide the basis for s–d scattering, which, for example, has been discussed extensively in the case of transition metal doped II–VI compound semiconductors [33, 34]. In the presence of a magnetic field, the alignment of the moment at cobalt sites would lead to spin splitting of the conduction band such that the up and the down spin electrons have different energy distributions [35]. Let the energy separation between the bottoms of the two subbands be $\delta(H)$. As δ increases, the distribution of the conduction electrons between the two subbands changes while conserving the total number of electrons. The energy splitting of the spin up and spin down bands can be written as $\delta = \delta_0(M/M_s)$, where δ_0 depends on the cobalt concentration, and M/M_s is the ratio of the magnetization (M) and its saturation value (M_s). The latter can be expressed by the phenomenological relation [36];

$$M/M_s = B_{3/2}[3\mu_B H/k_B(T+T_0)] \tag{2}$$

where $B_{3/2}$ is the Brillouin function for an $S = 3/2$ system and T_0 is a parameter which depends on the concentration of the transition metal ions. The MR in this scenario depends on the following factors whose relative strength is decided by energy scales, δ, k_BT, E_F, in addition to the energy dependence of the relaxation time and changes in the Thomas–Fermi screening radius of the ionized donors [35]. In the following we list some dominant contributions to the magnetoresistivity, and show how these contributions change *vis-à-vis* changes in temperature and strength of the magnetic field.

4.1. The magnetic field dependence of the scattering from non-magnetic impurities

A major contribution to the resistivity of a degenerate semiconductor comes from scattering by ionized dopant atoms. The scattering time τ_{im} can be estimated from the Brooks–Herring formula [37] combined with the Thomas–Fermi approximation for the effective impurity radius a_H [35]. The scattering time τ_{im} depends on the electron energy E, where E is measured from the bottom of the subband. As δ increases with the applied field, the electron redistribution raises the Fermi energy E_F in the majority spin subband and lowers E_F in the minority electron subband. A situation where $\tau_{im}(E)$ increases with the energy would lead to a negative MR because the dominant contribution to transport is from the majority electrons.

4.2. Interaction between mobile electrons and localized d orbitals

The s–d scattering makes a dominant contribution to the resistivity of dilute magnetic semiconductors in zero field. The external magnetic field affects the s–d scattering time τ_{sd} in two ways as discussed in detail by Shapira and Kautz [35]. First, the spins of magnetic

impurities become increasingly aligned in the presence of the field; this makes the scattering off these much more coherent, thereby increasing the τ_{sd}. Secondly, the number of final states available to the minority electrons for undergoing a spin flip scattering increases with the field as the Fermi level is pushed up in the spin-split (+) band. This effect saturates when $\delta \sim E_F$.

4.3. Modification of the Thomas–Fermi screening radius due to the exchange effect

When the conduction band splits, the screening of the ionized donors is mostly by the spin up electrons. Exchange effects then cause scattering of the up spin electrons to be stronger than that of down spin electrons. For large δ (stronger fields) one expects a positive MR due to this effect.

4.4. Electron–electron interaction effects

The dominant contribution to the conductivity of a degenerate three-dimensional system with $k_F l \gg 1$ in a magnetic field due to electron–electron interaction can be expressed as [28] $\Delta\sigma(H) = -AT^{1/2}g_3(h)$ for $h = g\mu_B H/k_B T \ll 1$, which is the case in hand. Here A is a positive constant and $g_3(h)$ has a limiting value of $0.053h^2$. With this definition of $g_3(h)$, the conductivity then becomes $\Delta\sigma(H) = -A(g\mu_B H)/T^{3/2}$. It is clear from this expression that the e–e interaction in our situation would lead to positive magnetoresistance quadratic in the magnetic field and suppressed strongly at high temperatures. The observation of a negative MR, which increases with field, suggests that in the temperature and field regime investigated here, e–e interaction corrections to MR are not significant.

4.5. Effects of phonon scattering on the MR

Since we are dealing with MR in the high temperature regime, magnetic field effects on the scattering of charge carriers by phonons cannot be neglected. In has been shown by Shapira and Kautz [35] that for degenerate statistics, which is the case in hand, phonons make a positive contribution to the MR.

4.6. Other manifestations of s–d scattering

The pronounced minimum in the resistivity of the samples with $x = 0.2$ and 0.3 is unlikely to occur due to localization as $k_F l$ is $\geqslant 1$ and the MR is predominantly isotropic. Further, the minimum cannot be attributed to extraneous effects such as tunnelling through grain boundaries [16] as these films do not show other features of grain boundary dominated transport such as activated mobility. Also, the feature is not present in cobalt-free films which have a similar microstructure. It was shown early on by Kondo that exchange interaction between conduction electrons and localized spins can lead to a minimum in the resistivity of a wide variety of dilute magnetic alloys [38]. The resistivity below this minimum varies as $\sim\gamma \ln T$ where γ is a negative constant, and this is followed by saturation at the lowest temperatures. The fundamental reason for the increase in the resistivity is the formation of a quasibound state between the magnetic impurity and the conduction electrons in its vicinity [38]. This bound state, with a coherence length of several tens of ångströms, prevails below a characteristic temperature T_K. The resistivity minimum followed by an increase in resistivity seen at low temperatures in samples with $x > 0.10$ is consistent with this picture.

The magnetoresistance of dilute magnetic alloys was calculated early on by Béal-Monod and Weiner [39] from the third-order perturbation expansion of the s–d exchange Hamiltonian. The dominant contribution to the MR at low fields in this theory goes as $\Delta\rho/\rho \sim \alpha M^2$, where

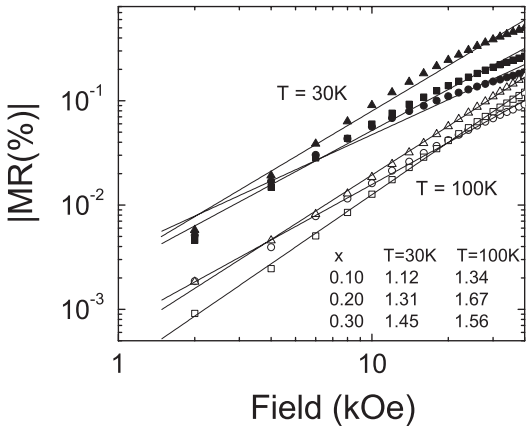

Figure 8. The low field magnetoresistance of $x = 0.10$, 0.20 and 0.30 samples at 30 and 100 K. The data have been plotted on a log–log scale. Straight lines are fits of the type $\Delta\rho/\rho \sim H^n$. The value of n for each curve is given in the figure.

α is a negative constant and M the magnetization. Since at low fields M is proportional to H, an H^2 field dependence of the MR is expected. Figure 8 shows the low field MR of all samples at 30 and 100 K on a log–log scale. While the power n of the $\Delta\rho/\rho \sim H^n$ fits remains less than 2, we see a systematic increase in the value of n with the cobalt concentration. At high fields where the magnetization tends to saturate, the theory predicts a transition to $-\ln H$ dependence of the MR. The transition is actually decided by the two energy scales $\mu_B g H$ and $k_B T$, where g is the Landé g-factor for the impurity moment. At higher temperatures the transition is expected to shift to the higher fields. The critical field H^* identified in figure 7 appears to separate the two regimes of behaviour.

Finally, a few observations on the nature of the Hall effect are in order. While the measurements on II–VI semiconductors such as CdS, CdTe with Mn or Co substitution at the group II element sites show strong effects of s–d exchange on magnetoresistance, no anomalous contribution to the Hall effect has been seen in these systems [33, 34]. These systems also do not show a long range ferromagnetic order. On the other hand, manganese doped GaAs shows long range FM ordering as well as an AHE at $T < T_{\text{Curie}}$ [40]. The anomalous Hall effect has also been reported in cobalt doped anatase and rutile $TiO_{2-\delta}$ films [41]. Again, a spontaneous magnetization is seen in these systems as well, although the origin of the magnetization lies in the presence of nanometre size cobalt clusters. The absence of AHE in our samples is consistent with the absence of a ferromagnetically ordered state even in samples where the existence of precipitates of CoO, which is a known antiferromagnet, is well established.

5. Conclusions

In summary, we have studied the effects of cobalt substitution at the Zn sites on the structure, resistivity, Hall coefficient and magnetoresistance of electron doped ZnO epitaxial films. Under the set of deposition conditions used here, the maximum solubility of Co in the wurtzite lattice of ZnO is 20%. While the solid solutions are devoid of any ferromagnetic ordering down to 10 K, the effects of s–d exchange are prominent in electron transport properties. These include a negative and predominantly isotropic magnetoresistance, which shows a power law dependence of the field followed by a log H field dependence at high fields, and a Kondo-like minimum in the resistivity. These films offer a model system for studying the effects of s–d exchange in a degenerate, wide band gap semiconductor.

Acknowledgment

This research was supported by a grant from the Defence Research and Development Organization, Government of India.

References

[1] For a recent review see Pearton S J, Abernathy C R, Overberg M E, Thaler G T, Norton D P, Theodoropoulou N, Hebard A F, Park Y D, Ren F, Kim J and Boatner L A 2003 *J. Appl. Phys.* **93** 1
[2] Ueda K, Hitoshi T and Tomoji K 2001 *Appl. Phys. Lett.* **79** 988
[3] Lim S-W, Hwang D-K and Myoung J-M 2003 *Solid State Commun.* **125** 231
[4] Prellier W, Fouchet A, Mersey B, Simon Ch and Raveau B 2003 *Appl. Phys. Lett.* **82** 3490
[5] Pakhomov A B, Roberts B K, Tuan A, Shutthanandan V, McCready D, Thevuthasan S, Chambers S A and Krishan K M 2004 *J. Appl. Phys.* **95** 7393
[6] Yoon S W, Cho S-B, We S C, Yoon S, Suh B J, Song H K and Shin Y J 2003 *J. Appl. Phys.* **93** 7879
[7] Sharma P, Gupta A, Rao K V, Owens F J, Sharma R, Ahuja R, Guillen J M O, Johansson B and Gehring G A 2003 *Nat. Mater.* **2** 673
Tiwari A, Jin C, Kvit A, Kumar D, Muth J F and Narayan J 2002 *Solid State Commun.* **121** 371
[8] Rao C N R and Deepak F L J 2005 *J. Mater. Chem.* submitted
[9] Risbud A S, Spaldin N A, Chen Z Q, Stemmer R and Seshadri S 2003 *Phys. Rev.* B **68** 205202
[10] Kolesnik S, Dabrowski B and Mais J 2004 *J. Appl. Phys.* **95** 2582
[11] Ando K, Saito H, Jin Z, Fukumura T, Kawasaki M, Matsumoto Y and Koinuma H 2001 *Appl. Phys. Lett.* **78** 2700
[12] Kim J H, Kim H, Kim D, Ikm Y E and Cho W K 2002 *J. Appl. Phys.* **92** 6066
[13] Lee E-C and Chang K J 2004 *Phys. Rev.* B **69** 085205
[14] See Chrisey D B and Hubler G K (ed) 1994 *Pulsed Laser Deposition of Thin Films* (New York: Wiley)
[15] Jacobs I S and Bean C P 1963 *Magnetism* vol 3, ed G T Rado and H Suhl (New York: Academic) p 271
[16] Chopra K L, Major S and Pandya D K 1983 *Thin Solid Films* **102** 1 and reference therein
[17] Kim H, Gilmore C M, Horwitz J S, Pique A, Murata H, Kushto G P, Schlaf R, Kafafi Z H and Chrisey D B 2000 *Appl. Phys. Lett.* **76** 259
[18] Bergman G 1979 *Phys. Today* (August) 25
[19] Chien C L and Westgate C R 1980 *Commemorative Symposium on Hall Effect and its Applications* (New York: Plenum)
[20] Berger L 1970 *Phys. Rev.* B **2** 4559
[21] Smit J 1958 *Physica* **24** 39
[22] Mott N F 1974 *Metal–Insulator Transitions* (London: Taylor and Francis) chapter 6
[23] Alexander M N and Holcomb D F 1968 *Rev. Mod. Phys.* **40** 815
[24] Roth A P and Williams D F 1981 *J. Appl. Phys.* **52** 6685
[25] Monod P 1967 *Phys. Rev. Lett.* **19** 1113
[26] Toyozawa Y 1962 *J. Phys. Soc. Japan* **17** 986
[27] Khosla R P and Fischer J R 1970 *Phys. Rev.* B **2** 4084
[28] Lee P A and Ramakrishnan T V 1985 *Rev. Mod. Phys.* **57** 287
[29] Bergman G 1984 *Phys. Rep.* **107** 1
[30] Kawabata A 1982 *Anderson Localization* ed Y Nagaoka and H Fukuyama (Berlin: Springer) p 122
[31] Bartholomew D U, Suh E K, Ramdas A K, Rodriguez S, Debska U and Furdyna J K 1989 *Phys. Rev.* B **39** 5865
[32] Lewicki A, Schindler A I, Miotkowski I and Furdyna J K 1990 *Phys. Rev.* B **41** 4653
[33] Furdyna J K 1988 *J. Appl. Phys.* **64** R29 and references therein
[34] Shapira Y, Oliveira N F Jr, Becla P and Vu T Q 1990 *Phys. Rev.* B **41** 5931
[35] Shapira Y and Kautz R L 1974 *Phys. Rev.* B **10** 4781
[36] Gaj J A, Planel R and Fishman G 1979 *Solid State Commun.* **29** 435
[37] Fistul V I 1969 *Heavily Doped Semiconductors* (New York: Plenum)
[38] See Ehrenreich H, Seitz F and Turnbull D (ed) 1969 *Solid State Physics; Advances in Research and Applications* vol 23 (New York: Academic)
[39] Béal-Monod M-T and Weiner R A 1968 *Phys. Rev.* **170** 552
[40] Van Esch A, Van Bockstal L, De Boeck J, Verbanck G, van Steenbergen A S, Wellmann P J, Grietens B, Bogaerts B, Herlach F and Borghs G 1997 *Phys. Rev.* B **56** 13103
[41] Shinde S R, Ogale S B, Higgins J S, Zheng H, Millis A J, Kulkarni V N, Ramesh R, Greene R L and Venkatesan T 2004 *Phys. Rev. Lett.* **92** 166601